Available online at www.sciencedirect.com
SCIENCE DIRECT®
PERGAMON
International Journal of Heat and Mass Transfer 47 (2004) 135–147
International Journal of HEAT and MASS TRANSFER
www.elsevier.com/locate/ijhmt

Numerical and experimental analysis of chemical dehydration, heat and mass transfers in a concrete hollow cylinder submitted to high temperatures

S. Dal Pont [a,b,*], A. Ehrlacher [a]

[a] *Laboratoire d'Analyse des Matériaux et Identification, Ecole Nationale des Ponts et Chaussées, ENPC-LAMI, 6 et 8, Av. B.Pascal, Cité Descartes, 77455 Marne La Vallée Cedex 2, France*

[b] *Dipartimento di Costruzioni e Trasporti, Universitá di Padova, via Marzolo 9, 35131 Padova, Italy*

Received 10 October 2002

Abstract

This paper presents a thermo-hydro-chemical model for concrete at high temperatures. Non-linear phenomena, heat and mass transfers, evolution of the phases constituting the porous medium are taken into account in a full three phases coupled analysis. The proposed model does not take into account mechanical aspects, i.e. the solid skeleton is considered as rigid. An experimental set-up and a numerical simulation are also presented. A hollow cylinder has been heated up to 523.15 K (250 °C) on the internal side and submitted to gas pressure/temperature measurements. A numerical simulation of the cylinder has been performed, showing a good correlation with the experimental observations.

Keywords: Numerical and experimental analysis; Heat and mass transfers; Chemical dehydration; Concrete hollow cylinder

1. Introduction

The problem of a porous medium (i.e. concrete) subjected to high temperatures is of great interest in civil engineering. Nuclear plants/waste storage structures [1], safety evaluations during fire in tall buildings and the recent fires that have occurred in European tunnels have focused the attention of many researchers [2–4].

With high temperatures, many non-linear phenomena concerning the different phases constituting the porous media must be taken into account. Many authors have highlighted the necessity of a coupled model [5–8]: not only heat conduction and vapour diffusion must be considered, but also liquid water flow due to pressure gradients and capillary effects (due to interface curvature inside pores produced by surface tension that alters the equilibrium between liquid water and gas).

This paper focuses mainly on the thermo-hydro-chemical model presented in [9–12] taking into account thermal kinetics and three full phases. Mechanical aspects are not considered i.e. mechanical damage is considered not to have a primary importance.

The porous structure of concrete is subjected to strong alterations when exposed to high temperatures. Chemical decomposition of the cement paste (i.e. dehydration) introduces in concrete pores free liquid water and modifies microstructure geometry and transport properties [10]. Moreover during the dehydration process, considerable amounts of heat are consumed [13]. Permeability has a sharp increase above 378.15 K [13] i.e. when dehydration is considered to begin. Concrete is an hygroscopic material with a considerable portion of the pores belonging to the lower range of mesopores [13], meaning that during air/vapour diffusion, Knudsen effects must be considered [14]. Physical properties of

* Corresponding author. Address: Laboratoire d'Analyse des Matériaux et Identification, Ecole Nationale des Ponts et Chaussées, ENPC-LAMI, 6 et 8, Av. B.Pascal, Cité Descartes, 77455 Marne La Vallée Cedex 2, France. Fax: +33-1-64-15-37-41.

E-mail address: dalpont@lami.enpc.fr (S. Dal Pont).

0017-9310/$ - see front matter © 2003 Elsevier Ltd. All rights reserved.
doi:10.1016/S0017-9310(03)00381-8

Nomenclature

a_c, b_c	capillary curve coefficient [MPa], [–]
A_T, A_p	permeability law coefficients [–]
A_v, B_v	effective diffusion coefficients [–]
C	unit energy constants [$J\,kg^{-1}\,K^{-1}$]
D	gas diffusivity [$m^2\,s^{-1}$]
d	water dehydration per unit volume [$kg\,m^{-3}$]
F	mass flux per surface unit [$kg\,m^{-2}s^{-1}$]
g	structure coefficient [–]
ΔH	specific enthalpy of evaporation [$J\,mol^{-1}$]
H	Heaviside function [–]
h	enthalpy per unit mass [$J\,kg^{-1}$]
k	intrinsic permeability [m^2]
k_r	relative permeability [–]
M	molar mass [$kg\,mol^{-1}$]
m	mass per unit volume [$kg\,m^{-3}$]
n	relative permeability constant [–]
n_σ	surface tension coefficient [–]
p	pression [Pa]
q	heat flux per unit of surface of skeleton [$W\,m^{-2}$]
R	universal gas constant [$J\,mol^{-1}\,K^{-1}$]
RH	relative humidity [–]
S_l	liquid saturation [–]
T	temperature [K]
t	time [s]
u	internal energy per volume unit [$J\,m^{-3}$]
u_π	internal energy per mass unit [$J\,kg^{-1}$]

Greek symbols

α	heat exchange coefficient [$W\,m^2\,K^{-1}$]
χ	average curvature [m^{-1}]
δ	dehydration energy of concrete per unit volume at state 0 [$J\,kg^{-1}$]
η	viscosity [$kg\,m^{-1}\,s^{-1}$]
λ	thermal conductivity [$W\,m^{-1}\,K^{-1}$]
ϕ	porosity [–]
ρ	density [$kg\,m^{-3}$]
σ	surface tension [$N\,m^{-1}$]
τ	characteristic time of dehydration [s]

Subscripts and superscripts

0	reference state
$\dot{x}$	time derivative of x variable
∞	ambient
π	liquid water, vapour water, dry air
$\underline{x}$	x variable tensor
a	dry air
ag	aggregate
an	anhydrous
atm	atmospheric
c	capillary
cr	critic
eq	equilibrium
g	gas mixture
hyd	hydrate
l	liquid water
sat	saturated
v	vapour water
w	total water

fluids (liquid water and moist air) saturating the medium are also strongly temperature dependent [15].

The presented model takes into account all the mentioned phenomena, typical of concrete at high temperatures, and is valid below the critical point of water (i.e. 647.15 K). Above this limit, water does not exist as a liquid, capillary pressure loses its meaning and an extension of the theory is required [5,16,17].

The first part of the paper consists of a presentation of the coupled hygrothermal model for concrete at high temperatures: the original and the most significative equations of the model are here presented while the full algebraic-differential system is given in the appendix together with the whole set of variables, the constants used in the formulas and the values of the variables at reference state. In the next section we present how this model can be numerically handled through the finite volume method. In the following an experimental set-up is presented: a hollow cylinder has been heated up to the temperature of 523.15 K and its temperature/gas pressure fields have been monitored. Numerical results are then presented and discussed. Finally a comparison between the numerical results of the simulation and the experimental observations is given.

2. The mathematical model

The mathematical model used in the analysis considers concrete as a multiphase porous material, where the solid skeleton is filled with liquid water and gas. The model consists of three conservation equations (mass conservation of dry air, mass conservation of water, energy conservation of the whole medium) completed by an appropriate set of constitutive and state equations as well as some thermodynamic relationships.

The main frame of the mathematical model is based on the model presented by Mainguy et al. [12], completed by an appropriate set of equations for the description of concrete dehydration and the evolution of

its properties with temperature. The validation of the model is obtained neglecting these added terms. It is therefore possible to reproduce a concrete drying process; the results obtained are comparable to [12,18].

2.1. Microstructure description

In porous medium pores, water is usually present as a condensed liquid which, thanks to the surface tension, is separated from its vapour by a concave meniscus (capillary water). Capillary pressure is defined as the difference between gas pressure (i.e. air pressure p_a and vapour pressure p_v) and the liquid phase pressure p_l:

$$p_c = p_a + p_v - p_l \tag{1}$$

The equilibrium equation between liquid water and gas is given by means of the well-known Laplace equation:

$$p_g - p_l = 2\sigma(T)\chi \tag{2}$$

where χ represents the curvature of the interface between the capillary water and the gas phase inside the pores of the medium. Due to the curvature, the equilibrium vapour water pressure differs from the liquid water pressure and the relationship can be obtained by means of the Kelvin equation. Given the hypotheses of incompressible liquid water and vapour as a perfect gas, the equation can be expressed as a function of the saturation pressure of pure water (see Eq. (M-11)):

$$p_l = p_{sat}(T) + \frac{\rho_l RT}{M_l} \ln\left(\frac{p_v}{p_{sat}(T)}\right) \tag{3}$$

Meniscus curvature is therefore dependent on liquid water content, i.e. liquid saturation S_l, and vice versa. Moreover the surface tension of equilibrium between liquid water and gas mixture is temperature-dependent, meaning that changing the temperature, the equilibrium condition changes.

The capillary curve (i.e. the curve $p_c(S_l, T)$) is clearly fundamental for the realistic modelling of hygrothermal behaviour of concrete. It gives the pore size distribution of the porous media relating the size of the largest pore filled to the actual water content. The relationship must be determined through sorption tests at different temperatures. The following equation between capillary pressure and saturation for ordinary concrete and high performance concrete has been assumed:

$$p_c = \frac{\sigma(T)}{\sigma(T_0)} a_c \left(S_l^{-b_c} - 1\right)^{\left(1-\frac{1}{b_c}\right)} \tag{4}$$

where a_c and b_c are concrete coefficients determined experimentally from the porosimetry curve [19] and the surface tension is defined in Eq. (C-2).

2.2. Mass conservation

Masses per unit volume of skeleton for air, vapour and liquid water are defined as follows:

$$m_a = \rho_a \phi (1 - S_l) \tag{5}$$

$$m_v = \rho_v \phi (1 - S_l) \tag{6}$$

$$m_l = \rho_l \phi S_l \tag{7}$$

where $\rho_\pi(p_\pi, T)$ is the density of the π phase (see Eqs. (C-19)–(C-21)). Given the hypotheses of perfect gases, ρ_a and ρ_v depend on pressure and temperature (see Eqs. (C-19) and (C-20)).

Water mass conservation equation is particularly important. Due to dehydration, an important volume of free water is introduced in concrete in particular below 573.15 K. This quantity is taken into account through a water source term: the dehydration per unit volume d. The classical equation of water conservation must be therefore completed by this source term:

$$\dot{m}_w - \dot{d} + \mathrm{div}(\underline{F}_l + \underline{F}_v) = 0 \tag{8}$$

where m_w is total water mass per unit volume of skeleton, $\underline{F}_l(T, S_l, p_g, p_l)$ and $\underline{F}_v(T, S_l, p_v, p_a, \phi)$ are respectively liquid water and vapour water mass fluxes per unit of skeleton surface (see Eqs. (C-5) and (C-6)).

The set of mass conservation equations is finally completed by the air mass conservation equation:

$$\dot{m}_a + \mathrm{div}(\underline{F}_a) = 0 \tag{9}$$

where m_a is the air mass per unit volume of skeleton, $\underline{F}_a(T, S_l, p_v, p_a, \phi)$ is the air mass flux per unit of skeleton surface (see Eq. (C-4)).

The modification of the cement paste and the aggregates produces strong modification on concrete microstructure. As the cement paste is exposed to increasing temperatures, the following phenomena can be observed:

- Up to 378.15 K (i.e. 105 °C), free water is expelled; if heating is slow enough, at the conventional temperature of 378.15 K free water is considered as no longer present in concrete, otherwise this phenomena can continue up to about 500 K [20].
- After 378.15 K hydrates start the decomposition into anhydrous and water. In particular, calcium silicate hydrate (CSH) transforms into water and calcium hydroxide $Ca(OH)_2$. Up to 573.15 K the dehydration of CSH produces an important mass loss and strong alterations in concrete microstructure.
- After the temperature of 573.15 K, mass and water loss are less important, though the decomposition of hydrates continues (e.g. decomposition of calcium hydroxide at 573.15 K). These phenomena are not concerned in the proposed analysis; moreover above

the temperature of 647.15 K water does not exist anymore as a liquid, and an extension of the model is required [21].

The variable d is here proposed as an experimentally determined variable. It is important to observe that dehydration is not an instantaneous process and it needs some time to take place. Its evolution has been considered through the following formula [9,10]:

$$\dot{d} = -\frac{1}{\tau}(d - d_{\mathrm{eq}}(T)) \tag{10}$$

which takes into account the asymptotic evolution of dehydration through τ, characteristic time of mass loss, and d_{eq} the water mass created at the equilibrium at the temperature T (see Eq. (C-22)).

Water production and dehydration of concrete have a strong influence on transport phenomena. It is reasonable to suppose that these phenomena are therefore connected to the variable d. Schneider and Herbst [22] showed also that increasing temperature produces a change in porosity: this dependance is here given through the variable d. The evolution of porosity changes the geometry of the microstructure (i.e. the void space) but does not affect the hypothesis of rigid skeleton (i.e. the neglecting of mechanical aspects). In the presented model, an experimental relationship proposed by [9] and [10], taking into account the Le Chatelier contraction [23], is retained:

$$\phi = \phi_0 + 0.72 \cdot 10^{-3} d \tag{11}$$

2.3. Energy equations

Dehydration takes some time to take place, and its kinetics is important especially during the transitory phase. Starting from a reference state at ambient temperature T_0, we denote m^0_{an} and m^0_{hyd} the mass per volume unit of anhydrous and hydrates at the reference state, and m_{an} and m_{hyd} at the actual state. m_{an} and m_{hyd} can be expressed as a function of d given the dehydration chemical reaction. It is normally assumed that the hydration of 100 g of cement requires 20 g of water [23]; the following expression can be therefore written:

$$m_{\mathrm{hyd}} = m^0_{\mathrm{hyd}} - 6d \tag{12}$$

$$m_{\mathrm{an}} = m^0_{\mathrm{an}} + 5d \tag{13}$$

Internal energy per volume unit $u(T, p_{\mathrm{a}}, p_{\mathrm{v}}, \phi, S_{\mathrm{l}})$ can be defined summing the energies of all concrete components (air, vapour water, liquid water, hydrates, anhydrous and aggregates):

$$u = m_{\mathrm{a}}u_{\mathrm{a}}(T) + m_{\mathrm{v}}u_{\mathrm{v}}(T) + m_{\mathrm{l}}u_{\mathrm{l}}(T) + m_{\mathrm{hyd}}u_{\mathrm{hyd}}(T) + m_{\mathrm{an}}u_{\mathrm{an}}(T) + m_{\mathrm{ag}}u_{\mathrm{ag}}(T) \tag{14}$$

where u_π represent the internal energy per mass unit of the π phase. Substituting Eqs. (12) and (13) into Eq. (14) we obtain the final form for energy equation:

$$u = m_{\mathrm{a}}u_{\mathrm{a}}(T) + m_{\mathrm{v}}u_{\mathrm{v}}(T) + m_{\mathrm{l}}u_{\mathrm{l}}(T) + (m^0_{\mathrm{hyd}} - 6d)u_{\mathrm{hyd}}(T) + (m^0_{\mathrm{an}} + 5d)u_{\mathrm{an}}(T) + m_{\mathrm{ag}}u_{\mathrm{ag}}(T) \tag{15}$$

This expression requires the knowledge of the internal energy of every phase at the reference state. These values cannot be directly measured, though it is possible to obtain a relationship among them (see Eq. (C-17)).

The energy equation takes into account the energetic phenomena related to water evaporation as well as dehydration i.e. the main phenomena occurring in concrete when temperature raises.

If evaporation occurs, water vapour mass Δm_{v} is created and the variation of internal energy is as follows:

$$\Delta u = \Delta m_{\mathrm{v}}(u_{\mathrm{v}}(T) - u_{\mathrm{l}}(T)) \tag{16}$$

When dehydration Δd occurs, free water is released inside concrete. Being concrete temperature higher than the boiling point, the free water released transforms partly into liquid water (Δm_{w}) and partly into vapour water (Δm_{v}); internal energy variation is as follows:

$$\Delta u = \Delta m_{\mathrm{v}}u_{\mathrm{v}}(T) + (\Delta d - \Delta m_{\mathrm{v}})u_{\mathrm{l}}(T) - 6\,\Delta d u_{\mathrm{hyd}} + 5\,\Delta d u_{\mathrm{an}} \tag{17}$$

Finally energy evolution is taken into consideration through a classical conservation equation:

$$\dot{\boldsymbol{u}} + \mathrm{div}(h_{\mathrm{a}}\underline{F}_{\mathrm{a}} + h_{\mathrm{v}}\underline{F}_{\mathrm{v}} + h_{\mathrm{l}}\underline{F}_{\mathrm{l}} + \underline{q}(T)) = 0 \tag{18}$$

where $q(T)$ is the heat flux per unit of surface of material (see Eq. (C-7)) and $h_\pi(p_\pi, T)$ is the enthalpy per unit mass of the π phase (see Eq. (C-3)).

2.4. Initial and boundary conditions

For model closure it is further necessary to define the initial and boundary conditions. The initial state specifies the variables of the problem at $t = 0$ giving the initial conditions required for the solution of the differential-algebraic system:

$$T = T_0 \tag{19}$$

$$p^0_{\mathrm{a}} + p^0_{\mathrm{v}} = p^0_{\mathrm{g}} \tag{20}$$

$$p^0_{\mathrm{v}} = \mathrm{RH} \times p_{\mathrm{sat}}(T_0) \tag{21}$$

$$d = d_0 \tag{22}$$

$$\phi = \phi_0 \tag{23}$$

where T_0, p^0_{g}, d_0, ϕ_0 are given in the annexe and RH is the relative humidity. The initial values for the remaining variables are calculated by substitution in Eqs. (M-5)–(M-11). Reference values are specified in the Appendix

A. Concerning boundary conditions it is necessary to fix some conditions for gas pressure and temperature. Gas pressure has been fixed on both cold and heated surface (first kind or Dirichlet's boundary conditions):

$$p_a + p_v = p_g^0 \tag{24}$$

On the cold side the heat convected from the surface of concrete is given by [10] (third kind, or Cauchy's mixed boundary conditions):

$$\underline{q}(T)\underline{n} = \alpha(T - T_\infty) \tag{25}$$

where $T_\infty = 293.15$ K is the temperature in the far field of undisturbed conditions, α is the exchange coefficient and $\underline{n}$ is the vector normal to the surface. Finally, on the internal face the thermal load has been imposed:

$$T(t) = T_0 + \dot{T}t \tag{26}$$

where $\dot{T} = 5$ K/h is the heating velocity. The discretization of the boundary conditions is required on the border elements. The nodes are at the interface porous media-external environment and the control volumes have been reduced to half size the internal volumes.

3. Results and discussion

3.1. The experimental set-up

The experiment has been performed on a hollow cylinder heated from the internal side, equipped with temperature and pressure sensors for the monitoring of the behaviour of concrete.

The cylinder (Fig. 1) is 1.5 m in height with an internal radius of 0.25 m and an external of 0.55 m. The cylinder dimensions have been chosen aiming at reproducing a real structure e.g. a wall of 30 cm of thickness. The concrete used in the analysis is an ultra high strength concrete of M100 type whose general characteristics at reference state are presented in [4]. The influence of permeability on concrete behaviour and on all transport phenomena is well known: following the guide lines proposed in [24], permeability has been measured at the reference temperature T_0 by means of a Cembureau permeability apparatus and its value is equal to 2×10^{-17} m^2.

Concerning temperature measurements it has been used a standard thermocouple of type K e.g. [4] or [9].

For what concerns the monitoring of gas pressures, the bibliography proposes a wide variety of sensors (e.g. [4]). The main problem of pressure gauges is related to their dimensions and to the influence they have on the measure itself of gas pressure. The sensor is an external element to concrete and constitutes a local discontinuity in the behaviour of concrete. It is therefore important to use sensors as small as possible taking also into account

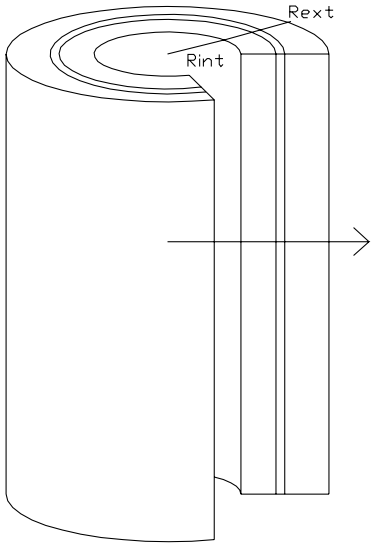

Fig. 1. Hollow cylinder.

their reliability in severe conditions i.e. high temperatures. Another problem related to pressure sensors is their correct positioning inside concrete for avoiding the measure of false pressure values. Generally speaking it is not possible to verify the correctness of positioning a priori: only the analysis of the obtained results can give some additional information.

In our analysis it has been used a cylindrical sensor type of 3 cm in height and 1.5 cm in diameter. Owing to their high cost only four pressure sensors have been used (placed at 3, 9, 16 and 25 cm from the heated surface).

The gauge at 9 cm has been excluded from the analysis given the fact that the measured pressure correspond to the vapour saturation pressure i.e. probably due to the formation of an air sack on the head of the sensor during its implantation which probably produced a "pressure cooker" effect.

The cylinder has been heated on the internal face up to the temperature of 523.15 K, with a 5 K/h velocity. The heat load has been therefore applied starting from an ambient temperature of 293.15 K and the final required temperature has been held for 30 days. The external face could freely exchange heat with the external environment. Day–night cycles had a non-negligible influence during the heating of the cylinder especially during the early phase of heating (Fig. 2). The gauges have been monitored during the whole test and the results registered regularly.

3.2. Numerical results

3.2.1. Numerical method

The hollow cylinder has been discretized using a finite volume scheme. Using the axial symmetry of the

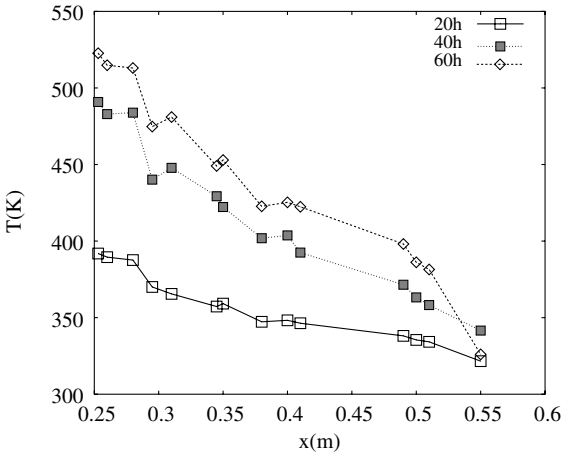

Fig. 2. Temperature vs. radius.

problem, the cylinder has been represented through its radius i.e. fluxes are considered to take place only in radial direction. The study has been therefore reduced to the study of a thin slice taken from the middle of the cylinder, switching from a 3D problem to a 1D pure radial problem i.e. phenomena in the perpendicular direction are considered negligible. The discretization method is the same proposed by [12]; the radius has been discretized through a grid of nodes, around which the control volumes have been built. The volume surface of two adjacent nodes is in common and it is through this surface that the fluxes are evaluated. This method has the main advantage of preserving the conservation equations in every volume, regardless of the volume shape and dimension.

In particular the hollow cylinder has been discretized through 11 volumes; this number has been chosen as a good compromise between the time required for calculation and the accuracy of results. A greater number of volumes has not given significant improvements in the results, though the time required for the solution of the system of equations slightly increases. The differential-algebraic system has been finally solved through the well-known DASSL algorithm [25]. Concerning the time step adopted, the DASSL algorithm implemented in Scilab, does not require a specific definition of Δt. Time step size is calculated according to predictor–corrector criteria; this leads to an increased velocity in the convergence. Further details are given in e.g. [25].

3.2.2. Numerical results

Numerical results at time stations $t = 10$, 20, 30, 40, 50, 60 h are here presented.

Below the boiling point of water, mass transport in concrete is quite low due to the not so strong pressure gradients. Free moisture, both vapour and liquid, tends to migrate towards the colder zones, and a consequent increase in liquid saturation and liquid water is present in the external layers of the cylinder.

When concrete temperature surpasses the conventional limit of 378.15 K i.e. 105 °C (at this temperature free water is considered to be no longer present in concrete), all the phenomena become more important.

Free liquid water boils off and the dehydration process begins with a strong mass loss and, as a consequence, a rapid evolution of the physical characteristics of the material. Due to the increased pressure gradient, the free moisture tends to diffuse towards the colder zones of the hollow cylinder. Being concrete permeability very low to water vapour, and even lower to liquid water, moisture cannot escape as rapidly as it is released, and the pore pressure rises substantially (Fig. 3).

The maximum pressure peak increases gradually up to about 3 atm at $t = 38$ h i.e. when the maximum temperature is reached. The desaturation front, which corresponds to the gas pressure peak (Fig. 4), migrates towards the external colder layers of the cylinder as the heat front moves inside concrete (Fig. 6). At the same time, water content and saturation increase in the zones behind the front.

All these phenomena are coupled with the evolution of the microstructure. The model does not take into account mechanical aspects, and in particular the damaging effect i.e. microcracks caused by differential thermal expansion are not modelled. The evolution of mass/heat transport properties are taken into account through porosity (Eq. (M-6)) and permeability evolution (Eq. (C-26)). Dehydration decomposes concrete and modifies microstructure geometry i.e. porosity augments with rising temperature (Fig. 5). Once completed the heating phase, the temperature field becomes stationary after

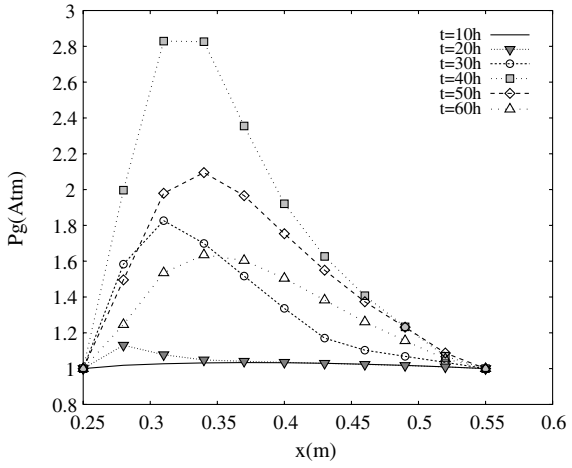

Fig. 3. Gas pressure vs. radius.

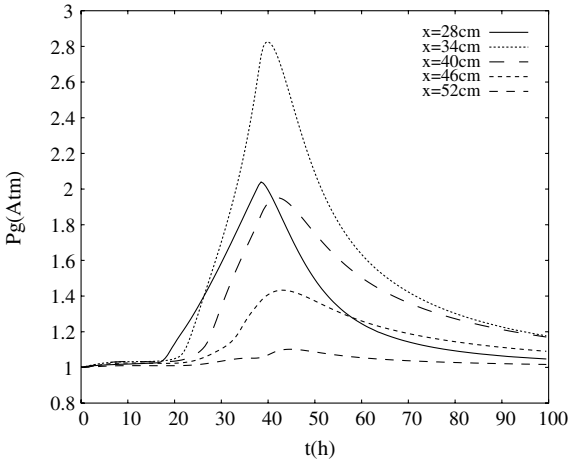

Fig. 4. Gas pressure vs. time.

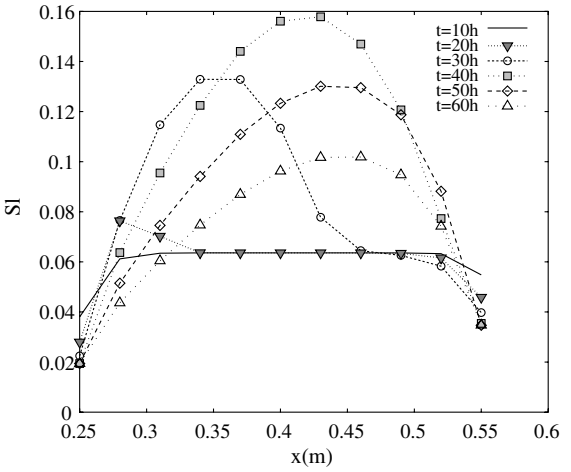

Fig. 6. Liquid saturation vs. radius.

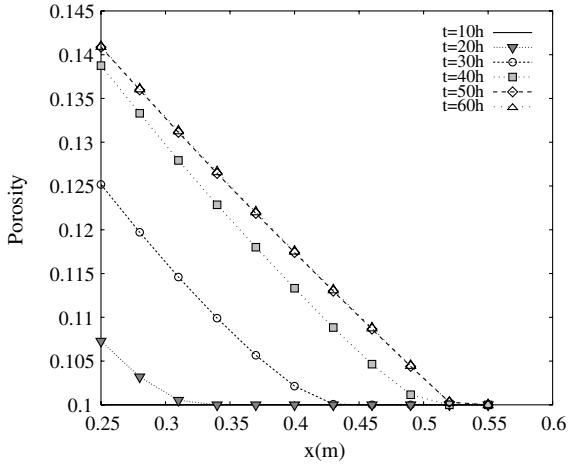

Fig. 5. Porosity vs. radius.

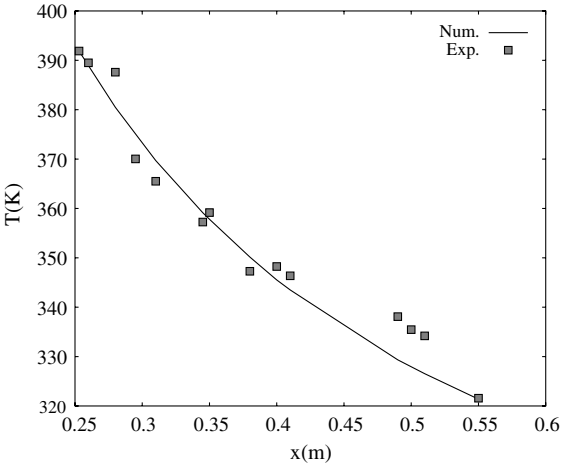

Fig. 7. Temperature vs. radius at $t = 20$ h.

$t = 60$ h, while the evolution of the other fields continues. Once ceased the water creation due to dehydration, the gas pressure peak reduces while continuing its migration, and saturation/water content decreases gradually due to moisture transport.

3.3. Experimental and numerical results: comparison

Temperature profiles show a good correlation with experimental results. During the transitory phase, some differences are present due to a non-uniform heating in the most external slice of the sample: i.e. day–night cycles had a non-negligible influence during the heating of the cylinder. As expected, these small perturbations are not appreciable at equilibrium (Figs. 7–9). The physical phenomena occurring inside the cylinder are characterized by a front of desaturation and a migration of water towards the colder zones, while at the same time a change of the parameters is observed moving towards the inner side of the structure (e.g. see Fig. 5 or 6). As it could be expected, the greatest changes are located in the area closer to the heat source, where temperature and pressure reach the highest values. Desaturation is present in spite of the high water production that takes place when the temperature is above 378.15 K due to concrete dehydration; desaturation is caused by a rapid evaporation of water, resulting in formation of a zone of increased water vapour content. As expected the maximum peak of vapour pressure moves towards the external colder part of the cylinder, following the free moisture migration.

Lacking the data of the pressure gauge at 9 cm from the heated surface, a comparison between the numerical

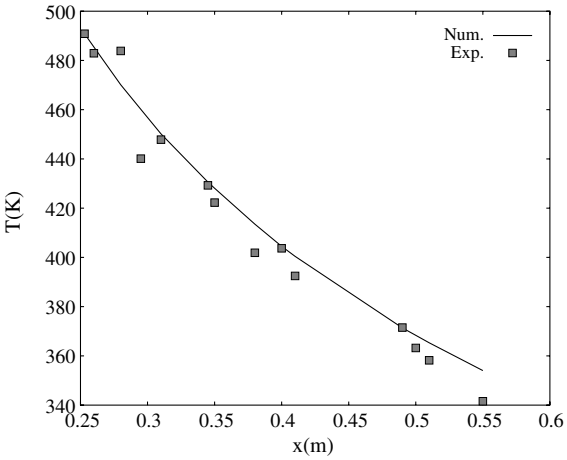

Fig. 8. Temperature vs. radius at $t = 40$ h.

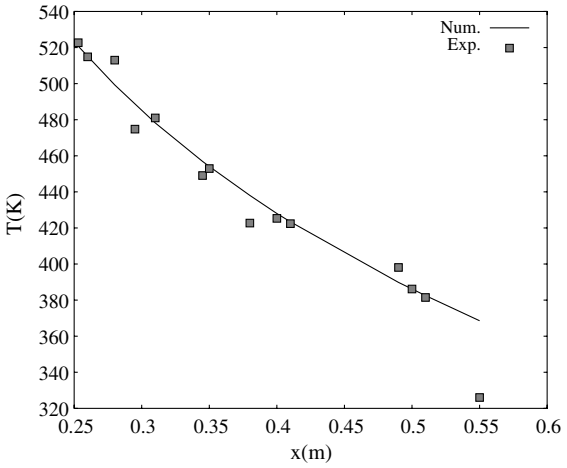

Fig. 9. Temperature vs. radius at $t = 60$ h.

and the experimental results is possible only on the three remaining sensors. Correlation is good, though on the third sensor placed at 16 cm a low pressure is measured (Figs. 10–12).

Many reasons can be given for explaining the non-perfect correspondence between experimental and numerical results on pressure field. The phenomena inside concrete, when high temperatures occur, are rather complex and it is not easy to measure and reproduce them. The measurements have been probably affected by a non-perfect installation and/or the influence the sensors have on the behaviour of concrete. Moreover the proposed model is relatively simple; the use of specific phenomenological laws for the high performance concrete used in the experimental test should improve the quality of results. Being these tests on the material quite expensive, some general equations for concrete have been adopted e.g. Eq. (C-9).

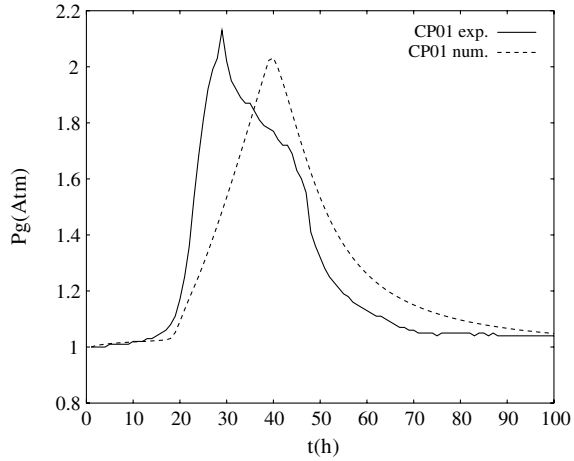

Fig. 10. Numerical and experimental gas pressure on sensor 1 (3 cm).

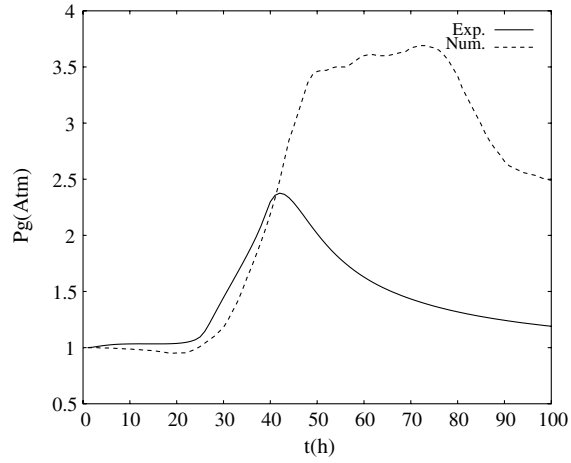

Fig. 11. Numerical and experimental gas pressure on sensor 3 (16 cm).

Nevertheless the model is able to predict, even if only qualitatively, the global behaviour of concrete and the gas pressure field.

4. Conclusions and perspectives

The developed model has allowed a qualitative description of the complex phenomena occurring in concrete at high temperatures. The main features of the model are the treatment of heat transfer together with liquid/vapour transport and air migration in the porous media. High temperatures effects have been considered through temperature/pressure dependance of many parameters by means of phenomenological expressions

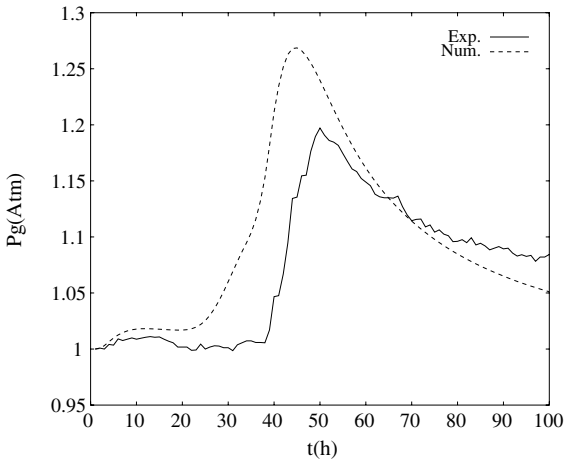

Fig. 12. Numerical and experimental gas pressure on sensor 4 (25 cm).

widely validated. An experimental set-up has been presented together with the related temperature and pore pressure measurements. The subsequent numerical analysis has showed qualitatively acceptable results, comparable to the observed data, allowing a deeper understanding of concrete at high temperatures. A further step of this research is the evaluation of the mechanical performances of concrete, including damage effects, and the implementation of the governing equations by means of a finite element procedure for more flexibility in space discretization by the use of the Hitecosp code presented in e.g. [3] or [21].

Appendix A

A.1. Equations of the model

In the model it has been chosen to introduce 11 variables: d, m_a, u, m_v, m_l, p_v, p_a, p_l, ϕ, S_l, T.

It is clear that this number can be easily reduced. Despite this it has been chosen not to reduce the system in order to preserve the readability of the system and the possibility of easily substituting one or more of the equations.

$$\dot{u} + \mathrm{div}(h_a \underline{F}_a + h_v \underline{F}_v + h_l \underline{F}_l + \underline{q}(T)) = 0 \tag{M-1}$$

$$\dot{m}_a + \mathrm{div}(\underline{F}_a) = 0 \tag{M-2}$$

$$\dot{m}_w - \dot{d} + \mathrm{div}(\underline{F}_l + \underline{F}_v) = 0 \tag{M-3}$$

$$\dot{d} = -\frac{1}{\tau}(d - d_{eq}(T)) \tag{M-4}$$

$$u = m_a u_a(T) + m_v u_v(T) + m_l u_l(T) + (m^0_{hyd} - 6d) u_{hyd}(T) + (m^0_{an} + 5d) u_{an}(T) + m_{ag} u_{ag}(T) \tag{M-5}$$

$$\phi = \phi_0 + 0.72 \cdot 10^{-3} d \tag{M-6}$$

$$p_a + p_v - p_l = \frac{\sigma(T)}{\sigma(T_0)} a_c (S_l^{-b_c} - 1)^{\left(1-\frac{1}{b_c}\right)} \tag{M-7}$$

$$m_a = \rho_a \phi (1 - S_l) \tag{M-8}$$

$$m_v = \rho_v \phi (1 - S_l) \tag{M-9}$$

$$m_l = \rho_l \phi S_l \tag{M-10}$$

$$p_l = p_{sat}(T) + \frac{\rho_l R T}{M_l} \ln\left(\frac{p_v}{p_{sat}(T)}\right) \tag{M-11}$$

The main system is completed by an appropriate system of complementary equations describing the different phases and their properties. The saturation pressure can be calculated from the Clausius–Clapeyron equation (C-1) or from empirical correlations e.g. the Hyland–Wexler formula.

$$p_{sat}(T) = p_{atm} \exp\left(\frac{\Delta H}{R} \frac{T - 373.15}{373.15 T}\right) \tag{C-1}$$

The surface tension gives the equilibrium tension between liquid water and gas inside pores. The following expression has been retained [26]

$$\sigma(T) = \sigma_0 \left(1 - \frac{T}{T_{cr}}\right)^{n_\sigma} \tag{C-2}$$

Enthalpies per unit mass are defined according to the classical definition:

$$h_\pi = u_\pi + \frac{p_\pi}{\rho_\pi} \tag{C-3}$$

Concerning the air and vapour fluxes some remarks must be made. The law describing the moisture transport in porous media is Fick's law associated with Darcy's law. These laws are separately well known, and the choice in favour of either a molar or a mass averaged mixture velocity formulation varies from author to author. This choice is often given without any explicit reasoning. Mainguy in [18] and [12] gives thermodynamic arguments for the choice of a molar based formulation. Flux equations are therefore the following:

$$\underline{F}_a = -\rho_a \left[\frac{\underline{k}(T) k_{rg}(S_l)}{\eta_g(T)} \underline{\mathrm{grad}}(p_a + p_v) + \left(1 + \frac{p_v}{p_a}\right) g D \underline{\mathrm{grad}}\left(\frac{p_a}{p_a + p_v}\right) \right] \tag{C-4}$$

$$\underline{F}_v = \rho_v \left[\frac{-\underline{k}(T) k_{rg}(S_l)}{\eta_g(T)} \underline{\mathrm{grad}}(p_a + p_v) + \left(1 + \frac{p_a}{p_v}\right) g D \underline{\mathrm{grad}}\left(\frac{p_a}{p_a + p_v}\right) \right] \tag{C-5}$$

$$\underline{F}_l = \frac{\rho_l}{\eta_l(T)} \underline{k}(T) k_{rl}(S_l) \underline{\mathrm{grad}}(p_l) \tag{C-6}$$

Heat flux is given by:

$$\underline{q}(T) = -\lambda \underline{\mathrm{grad}}(T) \tag{C-7}$$

The effective diffusion coefficient of vapour inside the pores of partially saturated concrete varies with saturation, temperature and gas pressure changes, and may be described as [22,27–29]:

$$D(\phi, S_\mathrm{l}, T, p_\mathrm{g}) = \phi(1 - S_\mathrm{l})^{A_\mathrm{v}} D_0 \left(\frac{T}{T_0}\right)^{B_\mathrm{v}} \frac{p_0}{p_\mathrm{g}} \tag{C-8}$$

In the chosen formulation, thermal conductivity of partially saturated concrete depends on the sole temperature. The Eurocode4 definition has been retained: this general equation is considered to take into account also condensation/vapourization influence on thermal conductivity:

$$\lambda(T) = 2 - 0.24\left(\frac{T-273}{120}\right) + 0.012\left(\frac{T-273}{120}\right)^2 \tag{C-9}$$

Internal energy of air and internal energy of water vapour are defined by means of the ideal gas assumption:

$$u_\mathrm{a}(T) = C_\mathrm{a} T \tag{C-10}$$

$$u_\mathrm{v}(T) = C_\mathrm{v} T \tag{C-11}$$

Internal energy of liquid water, u_l, is defined as follows [20]:

$$u_\mathrm{l}(T) = 4480(T - T_0) - 5.86 \times 10^{-7}\left(\frac{1}{T-715} - \frac{1}{T_0 - 715}\right) + 2.652 \times 10^5 \ln\left(\frac{T-715}{T_0-715}\right) + u_\mathrm{l}^0 \tag{C-12}$$

Harmathy [20] gives an approximated expression for concrete components (hydrate/anhydrous/aggregate) massive heat. Starting from this expression and considering hydrate as composed by CSH at 75% and portlandite at 25% [19], the following expression for hydrate energy has been obtained:

$$u_\mathrm{hyd}(T) = 946.6(T - T_0) + \frac{0.453}{2}(T^2 - T_0^2) - 150 \times 10^5\left(\frac{1}{T} - \frac{1}{T_0}\right) + u_\mathrm{hyd}^0 \tag{C-13}$$

The anhydrous is considered formed by C_2S [9]. The following expression has been obtained:

$$u_\mathrm{an}(T) = 838.9(T - T_0) + \frac{252 \times 10^{-4}}{2}(T^2 - T_0^2) - 14.13 \times 10^6\left(\frac{1}{T} - \frac{1}{T_0}\right) + u_\mathrm{an}^0 \tag{C-14}$$

Baroghel [19] gives also an expression for the aggregate energy:

$$u_\mathrm{ag}(T) = 180(T - T_0) + \frac{0.09}{2}(T^2 - T_0^2) + u_\mathrm{ag}^0 \tag{C-15}$$

Internal energy equation (M-5) can be rearranged in the following form:

$$u = m_\mathrm{a} u_\mathrm{a}(T) + m_\mathrm{v} u_\mathrm{v}(T) + m_\mathrm{l} u_\mathrm{l}(T) + m_\mathrm{hyd}^0 u_\mathrm{hyd}(T) + m_\mathrm{an}^0 u_\mathrm{an}(T) + m_\mathrm{ag} u_\mathrm{ag}(T) + d[-6(u_\mathrm{hyd}(T) - u_\mathrm{hyd}(T_0)) + 5(u_\mathrm{an}(T) - u_\mathrm{an}(T_0)) + u_\mathrm{l}(T_0)] - d[6u_\mathrm{hyd}(T_0) - 5u_\mathrm{an}(T_0) - u_\mathrm{l}(T_0)] \tag{C-16}$$

Internal energy of aggregates, anhydrous and hydrates at reference state cannot be directly measured. Though, it is possible to measure experimentally a relationship among these variables. Aggregate energy at reference state is considered negligible. The difference between the internal energies of hydrates and the internal energies of anhydrous and water at the reference temperature gives the constant δ whose value can be experimentally determined:

$$\delta = 6u_\mathrm{hyd}^0 - 5u_\mathrm{an}^0 - u_\mathrm{l}^0 = 2.5 \times 10^6 \ \mathrm{J\,kg^{-1}} \tag{C-17}$$

δ represents the required energy for the dehydration of CSH at the reference temperature.

We can therefore obtain the following expression for internal energy:

$$u = m_\mathrm{a} u_\mathrm{a}(T) + m_\mathrm{v} u_\mathrm{v}(T) + m_\mathrm{l} u_\mathrm{l}(T) + m_\mathrm{hyd}^0 u_\mathrm{hyd}(T) + m_\mathrm{an}^0 u_\mathrm{an}(T) + m_\mathrm{ag} u_\mathrm{ag}(T) + d[-6(u_\mathrm{hyd}(T) - u_\mathrm{hyd}(T_0)) + 5(u_\mathrm{an}(T) - u_\mathrm{an}(T_0)) + u_\mathrm{l}(T_0)] - \mathrm{d}\delta \tag{C-18}$$

The energy equation is defined given an additive constant. The definition of the constant is useless as we are interested in the variation of the internal energy.

Gas phases densities have been defined through the well known Clapeyron equation of state for ideal gases:

$$\rho_\mathrm{a} = \frac{p_\mathrm{a} M_\mathrm{a}}{RT} \tag{C-19}$$

$$\rho_\mathrm{v} = \frac{p_\mathrm{v} M_\mathrm{v}}{RT} \tag{C-20}$$

Liquid water density has been held constant; this hypothesis is acceptable due to the relatively low attained temperatures.

$$\rho_\mathrm{l} = \rho_\mathrm{l}^0 \tag{C-21}$$

$d_\mathrm{eq}(T)$ defines the water mass created at equilibrium; mass loss is reproduced through an exponential function, which is supposed a function of the sole temperature [9]:

$$d_{eq}(T) = \frac{7.5}{100} m_{eq}(378\ \mathrm{K}) \left[1 - \exp\left(-\frac{T-378}{200}\right)\right] \times H(T-378) \quad \text{(C-22)}$$

The porous space in concrete has a very complex inner structure which influences the vapour diffusion process. The simplest way of considering these effects is the introduction of the structure coefficient g. It takes into account an increase in the average path of the diffusing molecules which is caused by their tortuous course inside the pore space. Millington [30] expression is reproposed by means of the following expression:

$$g = \phi^{1/3}(1 - S_l)^{7/3} \quad \text{(C-23)}$$

Structure effect is taken into account also in Eq. (C-8): the term $\phi(1 - S_l)^{A_v}$, given $A_v = 1$, can be interpreted as the ratio of material volume occupied by the gas phase, while Eq. (C-23) can be interpreted as the sole term taking into account the tortuous course of diffusing molecules inside the pore space.

The liquid viscosity, which is considered as a function of the temperature [31], can be approximated using the Watson formula [32]:

$$\eta_l(T) = 0.6612(T - 229)^{-1.562} \quad \text{(C-24)}$$

Gas viscosity is considered temperature dependent [9]:

$$\eta_g(T) = 3.85 \times 10^{-8} T \quad \text{(C-25)}$$

Finally the set of equation is completed by the permeability relationships.

Intrinsic permeability is a material characteristic describing the penetration of gases or liquids through a porous material due to pressure head and it is generally determined by means of experimental tests using water or, more often, gas. During heating of concrete at high temperature complex physical and chemical processes take place, leading to inner structure changes, porosity increase and also intrinsic permeability augmentation [22].

In [22] Schneider and Herbst presented some results on changes of the inner structure and permeability, resulting from high temperature action, for four types of concrete. Results of these tests, concerning the effect of temperature and gas pressure on concrete intrinsic permeability, have been approximated by [21] by use of a formula of phenomenological type:

$$k(T, p_g) = k_0 \cdot 10^{A_T(T - T_0)} \left(\frac{p_g}{p_0}\right)^{A_p} \quad \text{(C-26)}$$

where A_T and A_p are constants depending on the type of concrete.

Intrinsic permeability is a characteristic of concrete skeleton, though gaseous and liquid phases have a different behaviour inside concrete. This means that another variable must be taken into consideration for describing the penetration of gas and liquid by means of the relative permeability. In particular Muskat and Meres [33] recommended the phase π permeability to be treated as isotropic and given by:

$$\underline{k}_\pi = \underline{k} k_{r\pi} \quad \text{(C-27)}$$

The relative permeability, similarly as for most capillary porous media, has been taken into consideration adopting the Van Genuchten [34] approach:

$$k_{rl}(S_l) = \sqrt{S_l}[1 - (1 - S_l^{1/n})^n]^2 \quad \text{(C-28)}$$

$$k_{rg}(S_l) = \sqrt{1 - S_l}(1 - S_l^{1/n})^{2n} \quad \text{(C-29)}$$

where n is an experimentally determined parameter (see e.g. [18]).

A.2. Constants and initial values

In the following, the constants which have been used in the model are presented together with initial values of the variables used for posing the reference state 0.

Constant	Description	Value	References
α	Heat exchange coefficient	8 [W m^{-2} K^{-1}]	–
A_T; A_p	Permeability law coefficients	0.05 [–]; 0.368 [–]	[21]
A_v; B_v	Effective diffusion coefficients	1 [–]; 1.667 [–]	[14,35,36]
a_c; b_c	Capillary curve coefficients	46.9364 [MPa]; 2.0601 [–]	[19]
C_a	Air energy constant	717 [J kg^{-1} K^{-1}]	[15]
C_v	Vapour energy constant	1418 [J kg^{-1} K^{-1}]	[15]
D_0	Diffusion coefficient	2.55e^{-5} [m^2 s^{-1}]	[21]
δ	Dehydration energy at state 0	2.5×10^6 [J kg^{-1}]	–
ΔH	Specific enthalpy of evaporation	39583.85 [Jmol^{-1}]	[15]
k_0	Intrinsic permeability	2×10^{-17} [m^2]	–
m^0_{hyd}; m^0_{an}	Unit volume mass	420 [kg m^{-3}]; 0 [kg m^{-3}]	[19]
m^0_{ag}	Unit volume mass	1400 [kg m^{-3}]	[19]

(continued on next page)

Constant	Description	Value	References
m_{eq}	Equilibrium mass	210 [kg m^{-3}]	[9]
M_l; M_v	Molar mass	0.018 [kg mol^{-1}]	[15]
M_a	Molar mass	0.029 [kg mol^{-1}]	[15]
n	Relative permeability constant	0.51 [–]	[34]
n_σ	Surface tension coefficient	1.26 [–]	[26]
p_{atm}	Atmospheric pressure	101325 [Pa]	–
R	Universal gas constant	8.317 [J mol^{-1} K^{-1}]	[15]
RH	Relative humidity	0.5 [–]	–
ρ_l^0	Water density	998 [kg m^{-3}]	[15]
σ_0	Surface tension	155.8×10^{-3} [N m^{-1}]	[26]
τ	Characteristic time of dehydration	10800 [s]	[9]
T_∞	Temperature in the far field	293.15 [K]	–
T_{cr}	Critic temperature	647.15 [K]	–

Finally variables values at reference state are here presented:

Variable	Value
T_0	293.15 [K]
d_0	0 [kg m^{-3}]
ϕ_0	0.1 [–]
$p_a^0 + p_v^0$	101325 [Pa]
p_v^0	1300 [Pa]

The remaining variable initial values are calculated by substitution into the algebraic equations of the main system presented (M-5)–(M-11).

References

[1] G. Ranc, J. Sercombe, S. Rodrigues, C. Gatabin, Structural and local behaviour of reinforced highstrength mock-up subjected to high temperatures, in: Conf. Int. FRAMCOS, 2001.

[2] F. Ulm, O. Coussy, Z. Bazant, The "chunnel" fire.2: analysis of concrete damage, J. Eng. Mech. (1999) 283–289.

[3] B. Schrefler, P. Brunello, D. Gawin, C. Majorana, F. Pesavento, Concrete at high temperature with application to tunnel fire, Comput. Mech. (29) (2002) 43–51.

[4] P. Kalifa, F. Menneteau, D. Quenard, Spalling and pore pressure in hpc at high temperatures, Cement Concr. Res. (30) (2000) 1915–1927.

[5] R. Lewis, B. Schrefler, The Finite Element Method in the Static and Dynamic Deformation and Consolidation of Porous Media, J. Wiley & Sons, 1998.

[6] W. Gray, S. Hassanizadeh, General conservation equations for multiphase systems: 1. Averaging technique, Adv. Water Res. 2 (1979) 131–144.

[7] W. Gray, S. Hassanizadeh, General conservation equations for multiphase systems: 2. Mass, momenta, energy and entropy transfer, Adv. Water Res. 2 (1979) 191–203.

[8] W. Gray, S. Hassanizadeh, General conservation equations for multiphase systems: 3. Constitutive theory for porous media, Adv. Water Res. 3 (1980) 25–40.

[9] A. Feraille, Le rôle de l'eau dans le comportement á haute température des bétons, Ph.D. thesis, ENPC, Paris, 2000.

[10] A. Feraille, P. Tamagny, A. Ehrlacher, J. Sercombe, Thermo-hydro-chemical modelling of a porous medium submitted to high temperature: an application to an axisymmetrical structure, Math. Comp. Mod, in press.

[11] F. Pesavento, Non linear modelling of concrete as multiphase material in high temperature conditions, Ph.D. thesis, Universitá degli Studi di Padova, 2000.

[12] M. Mainguy, O. Coussy, R. Eymard, Modélisation des transferts hydriques isothermes en milieu poreux. Application au séchage des matériaux à base de ciment, LCPC, 1999.

[13] Z. Bazant, F. Whittmann, Creep and Shrinkage in Concrete Structures, J. Wiley & Sons, 1982.

[14] J.-F. Daian, Condensation and isothermal water transfer in cement mortar. Part 1—pore size distribution, equilibrium, water condensation, and imbibition, Transport Porous Media 3 (1988) 563–589.

[15] ASHRAE Handbook: Fundamentals, ASHRAE, 2001.

[16] P. Baggio, C. Bonacina, B. Schrefler, Some considerations on modeling heat and mass transfer in porous media, Transport Porous Media 28 (1997) 233–251.

[17] D. Gawin, B. Schrefler, F. Pesavento, Modelling of hygrothermal behavior and damage of concrete at temperature above the critical point of water, Int. J. Numer. Anal. Meth. Geomech. (26) (2002) 537–562.

[18] M. Mainguy, O. Coussy, V. Baroghel-Bouny, The role of air pressure in the drying of weakly permeable materials, J. Eng. Mech. 127 (2) (1998) 582–592.

[19] V. Baroghel-Bouny, Caractérisation microstructurale et hydrique des pâtes de ciment et des bétons ordinaires et á trés hautes performances, Ph.D. thesis, ENPC, Paris, 1994.

[20] T. Harmathy, Thermal properties of concrete at elevated temperatures, J. Mech., JMLSA 5 (1) (1970) 47–74.

[21] D. Gawin, C. Majorana, B. Schrefler, Numerical analysis of hygro-thermal behaviour and damage of concrete at high temperature, Mech. Cohes. Frict. Mater. 4 (1999) 37–74.

[22] U. Schneider, H. Herbst, Permeabilitaet und porositaet von beton bei hohen temperaturen, Deutscher Ausschuss fuer Stahlbeton (1989) 23–52.

[23] A. Folliot, M. Buil, La structuration progressive de la pâte de ciment, Presse de l'ENPC, Paris, 1982.

[24] A. Abbas, M. Carcasses, J. Ollivier, Gas permeability of concrete in relation to its degree of saturation, Mater. Struct. 32 (1999) 3–8.
[25] L. Petzold, in: R.S. Stepleman et al. (Eds.), A Description of DASSL: A Differential/Algebraic System Solver, Amsterdam, 1983.
[26] B. Le Neindre, Tensions superficielles des composés inorganiques et des mélanges, Techniques de l'ingénieur, 1993, article K476.
[27] P. Perre, A. Degiovanni, Simulation par volumes finis des transfers couplés en milieux poreux anisotropes: séchage du bois à basse et à haute température, Int. J. Heat Mass Transfer (33) (1990) 2463–2478.
[28] P. Baggio, C. Bonacina, M. Strada, Trasporto di calore e di massa nel calcestruzzo cellulare, La Termotecnica (12) (1993) 53–60.
[29] J. Selih, A. Sousa, T. Bremner, Moisture transport in initially fully saturated concrete during drying, Transport Porous Media (24) (1996) 81–106.
[30] R. Millington, Gas diffusion in porous media, Science (130) (1959) 100–102.
[31] R. Reid, J. Praunsnitz, E. Bruce, The Properties of Gases and Liquids, McGraw Hill, New York, 1987.
[32] H. Thomas, M. Sansom, Fully coupled analysis of heat, moisture and air transfer in unsaturated soil, J. Eng. Mech. (121) (1995) 392–405.
[33] M. Muskat, M. Meres, The flow of heterogeneous fluids through porous media, Physics (7) (1936) 346–363.
[34] M. Van Genuchten, A closed-form equation or predicting the hydraulic conductivity of unsaturated soils, Sci. Soc. Am. J. 44 (1980) 892–898.
[35] P. Forsyth, R. Simspon, A two phase two component model for natural convection in a porous medium, Int. J. Numer. Meth. Fluids (12) (1991) 665–682.
[36] E. Mason, L. Monchick, Survey of the equation of state and transport properties of moist gases, Humid. Moist. Measure. Control Sci. (3) (1965) 257–272.